Multibody System Dynamics **12:** 47–74, 2004.

Dynamic Analysis for Planar Multibody Mechanical Systems with Lubricated Joints

PAULO FLORES[1], JORGE AMBRÓSIO[2] and J. PIMENTA CLARO[1]
[1]*Departamento de Engenharia Mecânica, Universidade do Minho, Campus de Azurém, 4800-058 Guimarães, Portugal*
[2]*Instituto de Engenharia Mecânica (IDMEC), Instituto Superior Técnico, Av. Rovisco Pais, 1041-001 Lisboa, Portugal, E-mail: jorge@dem.ist.utl.pt,*
web page: http://www.lemac.ist.utl.pt/IDMEC/I/index.html

(Received 1 September 2003; accepted in revised form 27 February 2004)

Abstract. The dynamic analysis of planar multibody systems with revolute clearance joints, including dry contact and lubrication effects is presented here. The clearances are always present in the kinematic joints. They are known to be the sources for impact forces, which ultimately result in wear and tear of the joints. A joint with clearance is included in the multibody system much like a revolute joint. If there is no lubricant in the joint, impacts occur in the system and the corresponding impulsive forces are transmitted throughout the multibody system. These impacts and the eventual continuous contact are described here by a force model that accounts for the geometric and material characteristics of the journal and bearing. In most of the machines and mechanisms, the joints are designed to operate with some lubricant fluid. The high pressures generated in the lubricant fluid act to keep the journal and the bearing surfaces apart. Moreover, the lubricant provides protection against wear and tear. The equations governing the dynamical behavior of the general mechanical systems incorporate the impact force due to the joint clearance without lubricant, as well as the hydrodynamic forces owing to the lubrication effect. A continuous contact model provides the intra-joint impact forces. The friction effects due to the contact in the joints are also represented. In addition, a general methodology for modeling lubricated revolute joints in multibody mechanical systems is also presented. Results for a slider-crank mechanism with a revolute clearance joint between the connecting rod and the slider are presented and used to discuss the assumptions and procedures adopted.

Keywords: multibody dynamics, joint clearance, dry contact, lubricated joints

1. Introduction

The dynamic analysis of mechanical systems has been developed assuming, in general, that the kinematic joints are perfect, i.e., joints characterized by perfect adjustments, no wear or deformations, perfectly aligned pairs and no friction. However, the clearances are always present in the kinematic joints and are known to be sources for impact forces, which ultimately result in wear and tear of the joints. As a matter of fact, the impacts within the machine joints with clearances lead to the degradation of the overall system performance [1, 2]. The serious consequences of the clearance joints on the behavior of the mechanical systems have motivated various theoretical and experimental investigations over the last three

decades [3–7]. Most of them are referred to planar and unlubricated joints. Ravn [1] and Schwab [8] are among the few who have incorporated the lubrication effect at the clearance joints in the simulation of multibody systems. In these works, the mechanical systems used to demonstrate the methods proposed were four bar linkage and slider–crank mechanisms. However, modeling the dynamics of mechanical systems with clearance joints and imperfections is a challenging issue in multibody dynamics and much work still remains to be done to achieve satisfactory modeling tools.

A joint with clearance is included in the multibody system much like a revolute joint, which has the kinematic constraints, replaced by a pair of forces representing the journal-bearing contact. Therefore, the clearance in a revolute joint implies that the system to which this is applied has two extra degrees of freedom. The dynamics of the joint is then controlled by forces developed on the journal and bearing. Thus, while a perfect revolute joint in a multibody system imposes kinematic constraints, a revolute clearance joint leads to force constraints.

If there is no lubricant in the joint, impacts occur in the system and the corresponding impulse is transmitted throughout the multibody system. These impacts and the eventual continuous contact are described here by a force model that accounts for the geometric and material characteristics of the journal and bearing. The energy-dissipative effects are introduced in the joint through the contact force model and by friction forces that develop during the contact. In most of the machines and mechanisms, the joints are designed to operate with some lubricant fluid. The high pressures generated in the lubricant fluid act to keep the journal and the bearing surfaces apart. Moreover, the lubricant provides protection against wear and tear. The importance of the analysis of lubricated joints in the mutibody mechanical systems is obvious due to the demand for the proper design of the journal-bearings in many industrial applications. In general, multibody mechanical systems use journal-bearings in which the load varies in both magnitude and direction, which results in dynamically loaded journal-bearing.

In what concerns to the clearance modelization, there are, in general, three approaches to model mechanical systems with revolute clearance joints, namely:

- Massless link approach [9, 10], in which the presence of clearance at a joint is modeled by adding a massless link with a fixed length equal to the radial clearance, as it is shown inFigure 1a. This results in the mechanism having an additional degree of freedom. Furthermore, this model assumes that there is contact between the journal and bearing all the time, being unable to represent free flight trajectories. Hence, the resulting equations of motion are found to be highly nonlinear and complex to solve. Wu and Earles [10] used the massless link model to successfully predict the occurrence of contact loss in revolute joints of planar linkage mechanisms.

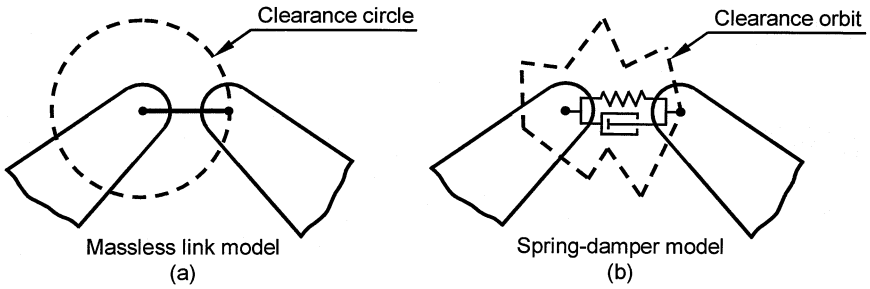

Figure 1. Examples of models for revolute joints with clearance: (a) massless link model; (b) spring-damper model.

- Spring-damper approach [5, 6], in which the clearance is modeled by introducing a spring-damper element, which simulates the surface elasticity as pictured in Figure 1b. This model does not represent well the physical nature of energy transfer process, and it is difficult to quantify the parameters of the spring and damper elements. Dubowsky [11] investigated the dynamic effects of clearance in planar mechanisms by simulating the elasticity of the contacting surfaces by linear springs and dampers.
- Momentum exchange approach [1, 12], in this model the journal-bearing elements are considered as two impacting bodies and contact forces controling the dynamics of the clearance joint.

Thus, in the massless link and spring-damper models, the clearance is replaced by equivalent components, which try to simulate the behavior of the clearance as closely as possible, whereas the momentum exchange approach is more realistic since the impact force model allows, with high level of approximation, to simulate the elasticity of the contacting surfaces as well as the energy dissipation during the impact.

The main emphasis of this paper is on the modeling and the clearance of revolute joints in multibody systems. Cartesian coordinates are used to describe the system components and the kinematic joints. The equations governing the dynamical behavior of the general mechanical systems incorporate the impact force due to the collision of the journal and the bearing, as well as the hydrodynamic forces owing to the lubrication effect. A continuous contact model, in which the local deformation and contact forces are treated as continuous, provides the intra-joint impact forces. For this model, it is assumed that material compliance and damping coefficients are available. The friction effects due to the contact in the joints are also modeled. In addition, a general methodology for modeling lubricated revolute joints in multibody mechanical systems is also presented. Results for a slider–crank mechanism with a revolute clearance joint between the connecting-rod and the slider are presented and used to discuss the assumptions and procedures adopted.

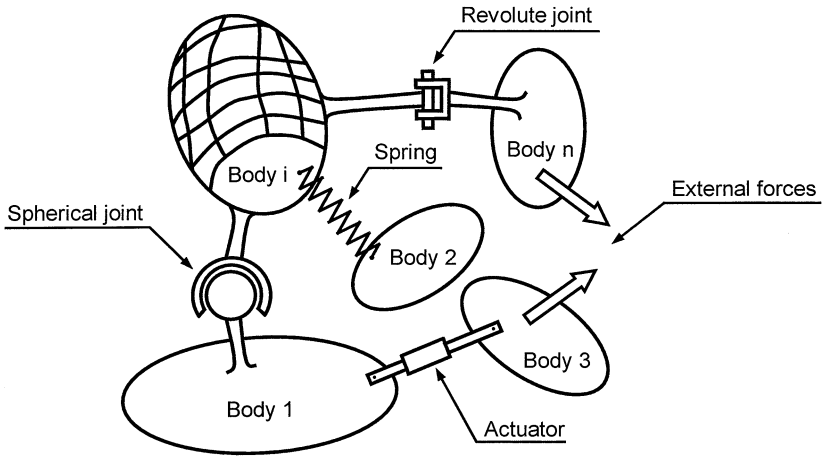

Figure 2. Schematic representation of a general multibody mechanical system.

2. Equations of Motion for Multibody Systems

To be able to analyze the transient response of a constrained dynamic system, it is first necessary to formulate the equations of motion that govern the behavior of the multibody system. Figure 2 depictsa multibody system (MBS), which consists of a collection of rigid and/or flexible bodies interconnected by kinematic joints and possibly some force elements. The forces applied over the system components may be the result of springs, dampers, actuators or external applied forces describing, gravitational, contact/impact or other forces. A wide variety of mechanical systems can be modeled in this way [13].

If the configuration of the MBS is described by n Cartesian coordinates $\mathbf{q}$, then a set of m algebraic kinematic independent holonomic constraints Φ can be written in a compact form as,

$$\mathbf{\Phi}(\mathbf{q}, t) = \mathbf{0} \tag{1}$$

Differentiating Equation (1) with respect to time yields the velocity constraint equation. After a second differentiation with respect to time the acceleration constraint equation is obtained

$$\mathbf{\Phi}_{\mathbf{q}}\dot{\mathbf{q}} = \upsilon \tag{2}$$

$$\mathbf{\Phi}_{\mathbf{q}}\ddot{\mathbf{q}} = \gamma \tag{3}$$

where $\mathbf{\Phi}_{\mathrm{q}}$ is the Jacobian matrix of the constraint equations, υ is the right side of velocity equations and γ is the right side of acceleration equations, which contains the terms that are exclusively function of velocity, position and time.

The equations of motion for a constrained MBS of rigid bodies are written as [13]

$$\mathbf{M}\ddot{\mathbf{q}} = \mathbf{g} + \mathbf{g}^{(c)} \tag{4}$$

where $\mathbf{M}$ is the system mass matrix, $\ddot{\mathbf{q}}$ is the vector that contains the state accelerations, $\mathbf{g}$ is the generalized force vector, which contains all external forces and moments and $\mathbf{g}^{(c)}$ is the vector of constraint reaction equations.

The joint reaction forces can be expressed in terms of the Jacobian matrix of the constraint equations and the vector of Lagrange multipliers as [14]

$$\mathbf{g}^{(c)} = -\boldsymbol{\Phi}_{\mathbf{q}}^{\mathrm{T}}\boldsymbol{\lambda} \tag{5}$$

where λ is the vector that contains m unknown Lagrange multipliers associated with m holonomic constraints. Substitution of Equation (5) in Equation (4) yields

$$\mathbf{M}\ddot{\mathbf{q}} + \boldsymbol{\Phi}_{\mathbf{q}}^{\mathrm{T}}\boldsymbol{\lambda} = \mathbf{g} \tag{6}$$

In dynamic analysis, a unique solution is obtained when the constraint equations are considered simultaneously with the differential equations of motion with proper set of initial conditions [13]. Therefore, Equation (3) is appended to Equation (6), yielding a system of differential algebraic equations that are solved for $\ddot{\mathbf{q}}$ and $\boldsymbol{\lambda}$. This system is given by,

$$\begin{bmatrix} \mathbf{M} & \boldsymbol{\Phi}_{\mathbf{q}}^{\mathrm{T}} \\ \boldsymbol{\Phi}_{\mathbf{q}} & \mathbf{0} \end{bmatrix} \begin{Bmatrix} \ddot{\mathbf{q}} \\ \boldsymbol{\lambda} \end{Bmatrix} = \begin{Bmatrix} \mathbf{g} \\ \boldsymbol{\gamma} \end{Bmatrix} \tag{7}$$

In each integration time-step, the accelerations vector, $\ddot{\mathbf{q}}$, together with velocities vector, $\dot{\mathbf{q}}$, are integrated to obtain the system velocities and positions at the next time-step. This procedure is repeated up to final time will be reached.

The set of differential algebraic equations of motion (7) does not use explicitly the position and velocity equations associated to the kinematic constraints, Equations (1) and (2), respectively. Consequently, for moderate or long time simulations, the original constraint equations are rapidly violated due to the integration process. Thus, to stabilize or keep under control the constraints violation, Equation (7) is solved by using the Baumgarte Stabilization Method [15], and the integration process is performed using a predictor-corrector [16] algorithm with variable step and order.

3. Model for Revolute Clearance Joints with Dry Contact

3.1. DEFINITION

The existence of clearance in the joints of mechanical systems is inevitable. Some clearance between the parts of mechanical systems is necessary to allow relative motion of the connected bodies, as well as to permit the assemblage of the mechanical systems. The clearance also exists due to manufacturing tolerances, imperfections, wear and material deformation. It is known that the performance of a MBS is degraded by the presence of clearance due to the impact forces, which contribute to bearing failure due to the shock loading, to reducing life, due to material fatigue, to generating high noise levels, causing energy dissipation and to excite unwanted vibratory responses.

In general, a clearance joint can be included in a multibody system much like a revolute joint. The classical approach, known as zero-clearance approach, considers that the connecting points of two bodies linked by a revolute joint are coincident. The introduction of the clearance in a joint separates these two points. Figure 3 depictsa revolute joint with clearance, that is, a journal-bearing. The difference in radius between the bearing and the journal defines the size of the radial clearance.

Although, a revolute joint with clearance does not constraint any degree of freedom from the mechanical system like the ideal joint, it imposes some kinematic restrictions, limiting the journal to move within the bearing. Thus, when clearance is present in a revolute joint, the two kinematic constraints are removed and two degrees of freedom are introduced instead. The dynamics of the joint is then controlled by forces working on the journal and the bearing. Thus, whilst a perfect revolute joint in a mechanical system imposes kinematic constraints, a revolute clearance joint leads to force constraints. When contact exists between the journal and bearing, a contact force is applied perpendicular to the plane of collision. The force is typically applied as a spring-damper element. If this element is linear, the approach is known as the Kelvin-Voigt model. When the relation is nonlinear, the model is generally based on the Hertz contact law [17].

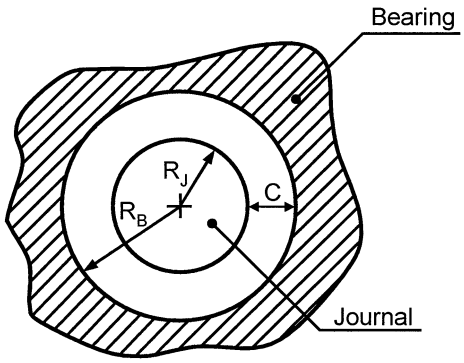

Figure 3. Revolute joint with clearance, that is, the so-called journal-bearing.

Over the last two decades several published research works have studied the different modes of motion of the journal inside the bearing [18, 19], namely:

- Contact or following mode, in this mode, the journal and the bearing are in contact and a sliding motion relative to each other is assumed to exist. In this mode, the penetration depth varies along the circumference of the journal. This mode is ended at the instant when the journal and bearing separate and the journal enters the free-flight mode.
- Free-flight mode, in which the journal moves freely within the bearing boundaries, i.e., the journal and the bearing joint are not in contact, hence there is no reaction force between these two elements.
- Impact mode, which occurs at the termination of the free-flight mode, impact forces are applied and removed. This mode is characterized by a discontinuity in the kinematic and dynamic characteristics, and a significant exchange of momentum occurs between the two impacting bodies.

During the dynamic simulation of a revolute joint with clearance, if the path of the journal center is plotted for each instant, these different modes of motion can be easily observed.

3.2. MATHEMATICAL MODEL

In order for the real joints to be used, it is necessary to develop a mathematical model for revolute clearance joints in the multibody mechanical systems. Figure 4 showstwo bodies *i* and *j* connected by a generic revolute joint with clearance. Part of body *i* is the bearing and part of body *j* is the journal. The center of mass of

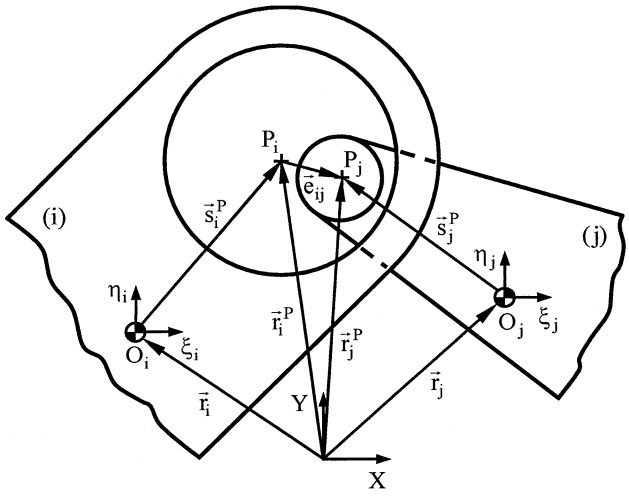

Figure 4. Generic revolute joint with clearance in a multibody mechanical system.

bodies i and j are O_i and O_j, respectively. Body-fixed coordinate systems $\xi\eta$ are attached at their center of mass, while the XY coordinate frame represents the global coordinate system. Point P_i indicates the center of the bearing, and the center of the journal is at point P_j.

In the dynamic simulation, the behavior of the revolute clearance joint is treated as an oblique eccentric impact between the journal and the bearing. The mechanics of this type of impact involve both relative normal velocity and tangential velocity. When impact occurs, an appropriate contact law is applied and the resulting forces are introduced as generalized forces in the equations of motion of the MBS.

From Figure 4, the eccentricity vector $\mathbf{e}_{ij}$, which connects the centers of the bearing and the journal, is calculated as,

$$\mathbf{e}_{ij} = \mathbf{r}_j^P - \mathbf{r}_i^P \tag{8}$$

where both $\mathbf{r}_j^P$ and $\mathbf{r}_i^P$ are described in global coordinates with respect to the inertial reference frame [13], that is,

$$\mathbf{r}_k^P = \mathbf{r}_k + \mathbf{A}_k \mathbf{s}'^P_k, (k = i, j) \tag{9}$$

The magnitude of the eccentricity vector is evaluated as,

$$e_{ij} = \sqrt{\mathbf{e}_{ij}^{\mathrm{T}} \mathbf{e}_{ij}} \tag{10}$$

The unit vector $\mathbf{n}$ normal to the surfaces of collision between the bearing and the journal is aligned with the eccentricity vector. This is written as,

$$\mathbf{n} = \frac{\mathbf{e}_{ij}}{e_{ij}} \tag{11}$$

The unit vector has the same direction as the line of centers of the bearing and the journal. With reference toFigure 5, the penetration depth due to the impact between the journal and the bearing is evaluated as

$$\boldsymbol{\delta} = e_{ij} - c \tag{12}$$

where c is the radial clearance, given as the difference between the radius of the journal and the radius of the bearing. Consequently, the radial clearance is specified quantity.

Let points Q_i and Q_j indicate the contact points on body i and j, respectively. Then, the position of the contact or control points Q_i and Q_j are evaluated as,

$$\mathbf{r}_k^Q = \mathbf{r}_k + \mathbf{A}_k \mathbf{s}'^Q_k + R_k \mathbf{n}, (k = i, j) \tag{13}$$

where R_i and R_j are the bearing and journal radius, respectively.

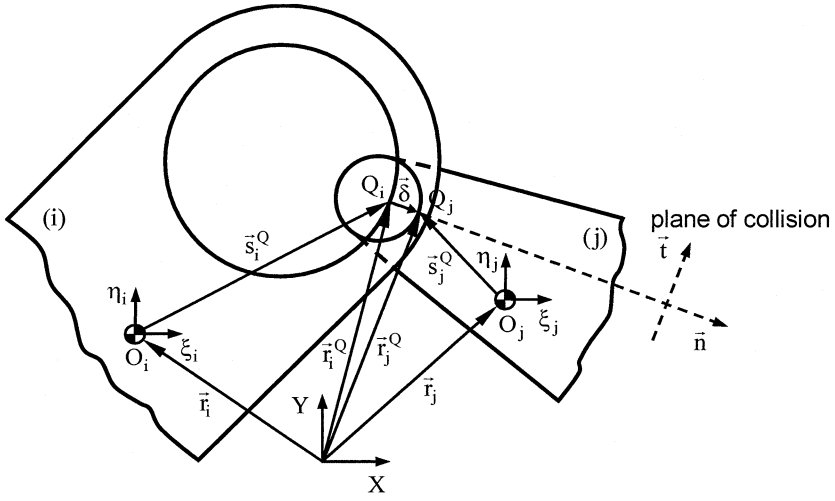

Figure 5. Penetration depth due to the impact between the bearing and the journal.

In some contact models, it is important to evaluate dissipative effects that develop during impact. In such models it is necessary to calculate the relative velocity between impacting surfaces. The velocity of the contact points Q_i and Q_j in the global coordinate system can be found by differentiating equation (13) with respect to time, yielding

$$\dot{\mathbf{r}}_k^Q = \dot{\mathbf{r}}_k + \dot{\mathbf{A}}_k \mathbf{s}_k'^Q + R_k \dot{\mathbf{n}}, \quad (k = i, j) \tag{14}$$

where $(\dot{\bullet})$ denotes the derivative with respect to the time of quantity $(\bullet)$.

The relative velocity of the contact points is projected onto the plane of collision, yielding a relative normal velocity, v_N, and a relative tangential velocity, $\mathbf{v}_T$, as shown in Figure 6. Thenormal relative velocity determines whether the contact bodies are approaching or separating. Similarly, the tangential relative velocity determines whether the contact bodies are sliding or sticking. The relative scalar velocities, normal and tangential to the plane of collision are found by projecting the relative impact velocity onto each one of these directions,

$$v_N = \left(\dot{\mathbf{r}}_j^Q - \dot{\mathbf{r}}_i^Q\right)^T \mathbf{n} \tag{15}$$

$$v_T = \left(\dot{\mathbf{r}}_j^Q - \dot{\mathbf{r}}_i^Q\right)^T \mathbf{t} \tag{16}$$

where $\mathbf{t}$ is obtained by rotating the normal vector $\mathbf{n}$ in the counter clockwise direction by 90°.

At the contact points work normal and tangential forces, $\mathbf{f}_N$ and $\mathbf{f}_T$, respectively. These forces can be evaluated using a contact force law and a friction law, for

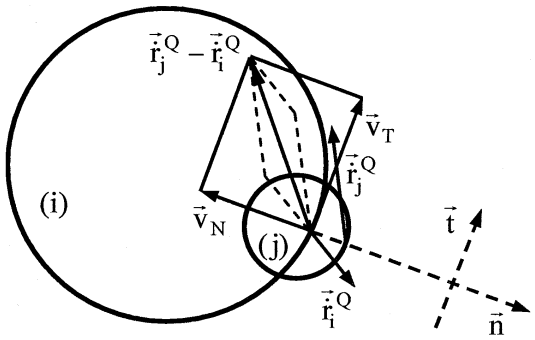

Figure 6. Velocities vectors of impact between the bearing and journal.

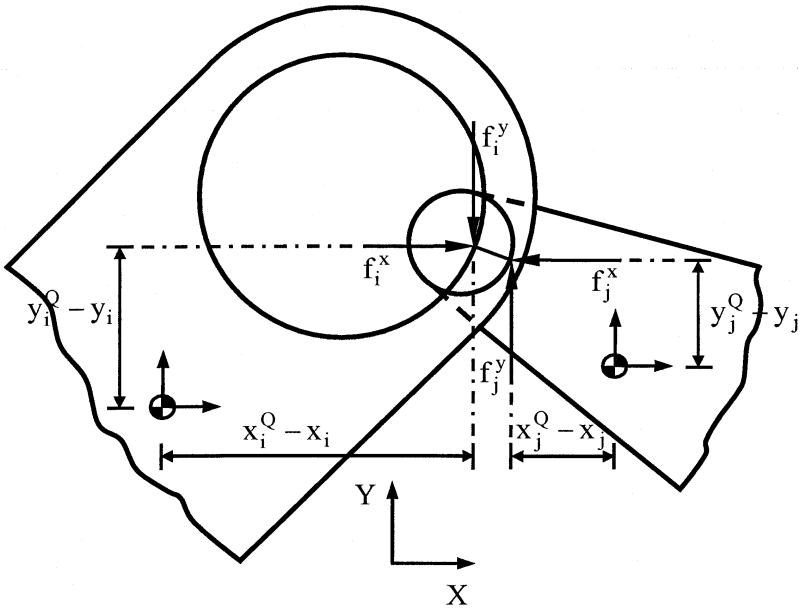

Figure 7. Force vectors that working at the points of contact.

example the Coulomb law. The contributions to the generalized vector of forces and moments, **g** in Equation (7), are found by projecting the normal force and tangential forces onto the X and Y directions. These forces that act on the contact points of bodies i and j are transferred to the center of mass of bodies, respectively. Referring toFigure 7, the forces and moments working on the center of mass of body $i$are given by,

$$\mathbf{f}_i = \mathbf{f}_N + \mathbf{f}_T \tag{17}$$

$$\mathbf{m}_i = -\left(y_i^Q - y_i\right)\mathbf{f}_i^x + \left(x_i^Q - x_i\right)\mathbf{f}_i^y \tag{18}$$

The forces and moments corresponding to the body j are written as,

$$\mathbf{f}_j = -\mathbf{f}_i \tag{19}$$

$$\mathbf{m}_j = \left(x_j^Q - x_j\right)\mathbf{f}_j^y - \left(y_j^Q - y_j\right)\mathbf{f}_j^x \tag{20}$$

The actual magnitudes of the forces are only dependent on the contact force model used.

3.3. CONTACT/IMPACT FORCE MODELS

To evaluate efficiently the contact forces between the bearing and journal, in a revolute joint with clearance, special attention must be given to the numerical description of the contact model. Information on the impact velocity, material properties of the colliding bodies and geometry characteristics of the surfaces in contact must be included into the force contact model. These characteristics are observed with a continuous contact force, in which the deformation and contact force are considered as continuous functions. Furthermore, it is important that the contact model can add to the stable integration of the MBS equation of motion.

The simplest contact force relationship, known as Kelvin-Voigt viscous-elastic model, is modeled by a parallel spring-damper element [20]. The spring represents the elasticity of the contacting bodies, and the damper describes the loss of kinetic energy during the impact. This model assumes that both the spring and damper are linear. When the contact bodies are separating from each other, the energy loss is included in the contact model by multiplying the rebound force with a coefficient of restitution. The normal Kelvin-Voigt contact force f_N, is calculated from penetration depth, δ, multiplied by a spring constant, K, yielding

$$f_N = \begin{cases} K\delta & \text{if} \quad v_N > 0 \quad \text{(loading phase)} \\ K\delta e & \text{if} \quad v_N < 0 \quad \text{(unloading phase)} \end{cases}, \tag{21}$$

where K is the spring stiffness, δ is the relative penetration depth, e is the restitution coefficient and v_{N} is the relative normal velocity of the colliding bodies. The main difficulty of this model deals with the quantification of the spring constant, which depends on the geometry and physical properties of contacting bodies. It is an oversimplification of the model to assume linear relation between penetration depth and contact force because the contact force depends on the shape of the surfaces in contact, the conditions of the surfaces, material properties, and so on, which suggests a relation of more complex nature.

The best-known contact force law between two spheres of isotropic materials is due to the pioneering work of Hertz, which is based on the theory of elasticity [21]. The Hertz contact theory is restricted to frictionless surfaces and perfectly elastic solids. The nonlinear normal contact force, known as the Hertz force-displacement

law, is evaluated as a function of indentation between two colliding bodies, as follows,

$$f_N = K\delta^n \tag{22}$$

where K is the generalized stiffness contact and δ is the relative normal indentation between the bodies. The exponent n is generally set to 1.5 for metallic surfaces. In other materials, such as glass or plastic, it can be either higher or lower. The generalized parameter K is dependent on the material properties and the shape of the contact surfaces. For two spheres in contact, the generalized stiffness coefficient is function on the radii of the spheres body i and j and the material properties as [22],

$$K = \frac{4}{3\pi(\sigma_i + \sigma_j)}\left[\frac{R_i R_j}{R_i - R_j}\right]^{\frac{1}{2}} \tag{23}$$

where the material parameters σ_i and σ_j are given by,

$$\sigma_k = \frac{1 - \nu_k^2}{\pi E_k}, (k = i, j) \tag{24}$$

variables ν_k and E_k are, respectively, the Poisson's ratio and the Young's modulus associated with the material of each sphere. It is important to note that the radius of the journal, body j, is inserted as negative value because of the opposite curvature of the impacting surfaces. It is apparent that the Hertz contact law given by Equation (22) cannot be used during both phases of contact, loading and unloading, since this model takes not into account the energy dissipation in the process of impact, i.e., this is a pure elastic contact model. The advantage of the Hertz law relative to Kelvin-Voigt model is its nonlinearity, that for the case of the parameter $n > 1$ penalizes the larger penetration.

Hunt and Crossley [23] represent the contact forces by the Hertz force-displacement law plus a nonlinear visco-elastic element. On the basis of Hunt and Crossley work, Lankarani and Nikravesh [17] developed a contact force model with hysteresis damping for impact in multibody systems. This model uses the general trend of Hertz contact law and a hysteresis damping function is incorporated, which represents the energy dissipation during the impact. In fact, when an elastic body is subjected to cyclic load, the energy loss in the material causes a hysteresis loop in the force-displacement diagram. The contact force including internal damping can be written as [17]

$$f_N = K\delta^n\left[1 + \frac{3(1 - e^2)}{4}\frac{\dot{\delta}}{\dot{\delta}^{(-)}}\right] \tag{25}$$

where the generalized parameter K can be evaluated by Equations (23) and (24), e is the restitution coefficient, $\dot{\boldsymbol{\delta}}$ is the relative penetration velocity and $\dot{\boldsymbol{\delta}}^{(-)}$ is the relative impact velocity. Equation (25) is only valid for impact velocities lower than the propagation velocity of elastic waves across the bodies, i.e., $\dot{\delta}^{(-)} \leq 10^{-5}\sqrt{E/\rho}$, where E is the Young modulus and ρ is the material mass density [24]. The velocity of wave propagation $\sqrt{E/\rho}$, is the larger of two propagation velocities of the elastic deformation waves in the colliding bodies. Impact at higher velocities, exceeding the propagation velocity of the elastic deformation waves, is likely to dissipate energy in a form of permanent indentation. Lankarani and Nikravesh [25] also proposed a new approach for contact force analysis, which includes permanent indentation. Indeed, at fairly moderate or higher velocities of colliding bodies, especially metallic solids, permanent indentations are left behind on the colliding surfaces. Hence, local plasticity of the surfaces in contact becomes the dominant source of energy dissipation during impact.

The contact models given by Equations (22) and (25) are only valid for impacts between colliding spheres. For an internal pin configuration, a literature search has failed to yield a force-displacement relationship for an elastic pin in a circular hole or the contact between two cylinders. Based on Hertz theory, Dubowsky and Freudenstein [6] presented an expression for the indentation as function of the contact force for the internal of a shaft inside a cylinder as,

$$\boldsymbol{\delta} = f_N\left(\frac{\sigma_i + \sigma_j}{L}\right)\left[\ln\left(\frac{L^m(R_i - R_j)}{f_N R_i R_j(\sigma_i + \sigma_j)}\right) + 1\right] \tag{26}$$

where R_{ij} and σ_{ij} represent the same quantities that appear in Equation (23), L is the length of the cylinder and the exponent m has a value 3. With the indentation depth, δ, known in Equation (26) it is necessary to employ an iterative scheme, such as Newton-Raphson method to solve it for the normal contact force f_N. An equation similar expression (26) was suggested by Goldsmith [22], but with exponent value of m equal to 1. This value, however, leads to a problem with the consistency of units. The ESDU-78035 Tribology Series [26] presented some expressions for contact mechanics analysis. For a circular contact the ESDU-78035 model is the same as the pure Hertz law. For rectangular contact, e.g., a pin inside a cylinder, the expression is,

$$\delta = f_N\left(\frac{\sigma_i + \sigma_j}{L}\right)\left[\ln\left(\frac{4L(R_i - R_j)}{f_N(\sigma_i + \sigma_j)}\right) + 1\right] \tag{27}$$

The cylindrical models presented above are purely elastic, i.e., no energy dissipation is accounted during impact process. Thus, Lankarani and Nikravesh contact force model given by Equation (25), which is valid only for colliding spheres, is largely used for cylindrical contacts own to its simplicity. An equivalent stiffness

value, obtained from using Equation (26) or (27), is used in Equation (25) in case of cylinder-to-cylinder contact.

3.4. FRICTION FORCE MODEL

In a multibody system, friction forces are likely to appear in joints where there are contacting surfaces belonging to different bodies that have a relative sliding motion. The Coulomb law [27] of sliding friction can represent the most fundamental and simplest model of friction between dry contacting surfaces. This law relates tangential and normal components of reaction force at the contact point by introducing a coefficient of friction, which acts if relative sliding occurs. The computer implementation of the Coulomb friction model in a general-purpose program can lead to numerical difficulties, as it is highly nonlinear and it can involve switching between sliding and stiction conditions. A consistent consideration of the Coulomb friction model can be found in some research papers devoted to subject [28, 29]. The dynamic friction force, in the presence of sliding, can be written as [30]

$$f_T = -c_f \, c_d \, f_N \frac{\mathbf{v}_T}{v_T} \tag{28}$$

where c_f is the friction coefficient, f_N is the normal force, v_T is the relative tangential velocity and c_d is a dynamic correction coefficient, which is expressed as,

$$c_d = \begin{cases} 0 & \text{if} \quad v_T \leq v_0 \\ \dfrac{v_T - v_0}{v_1 - v_0} & \text{if} \quad v_0 \leq v_T \leq v_1 \\ 1 & \text{if} \quad v_T \geq v_1 \end{cases} \tag{29}$$

The dynamic correction factor prevents that the friction force changes direction for almost null values of the tangential velocity, which is perceived by the integration algorithm as a dynamic response with high frequency contents, forcing to reduce the time-step size. The modified friction model represented by Equation (28) does not account for the adherence between the sliding contact surfaces.

3.5. NUMERICAL ASPECTS ASSOCIATED TO THE CONTACT ANALYSIS

As mentioned before in a revolute clearance joint three different types of motion between the journal and the bearing can be observed, namely: free flight motion, impact mode and continuous contact motion [19]. In dynamic simulation it is very important to find the precise instant of transition between these different sates. This requires close interaction with the numerical procedure to continuously detect and analyze all types of motion. If not, errors may built-up and the final results will be inaccurate.

When a system consists of fast and slow components, that is, the *eigenvalues* are widely spread, the system is designated as being stiff [13]. Stiffness in the system equations of motion arises, when the gross motion of the overall mechanism is combined with the nonlinear contact forces that lead to rapid changes in velocity and accelerations. In addition, when the equations of motion are described by a coupled set of differential and algebraic equations, the error of the response system is particularly sensitive to constraints violation. Constraints violation inevitably leads to artificial and undesired changes in the energy of the system. However, by applying a stabilization technique the constraint violation can be reduced and kept under control. During the numerical integration procedure, both the order and the step size are adjusted to keep the error tolerance under control. In particular, the variable step size of the integration scheme is a desirable feature when integrating systems that exhibit different time scales, such as in MBS with clearance joints. Thus, large steps are taken when the motion is controlled by free flight type and when impact occurs the step size is decreased substantially to capture the high frequency response of the system.

One of the most critical aspects in dynamic simulation of the MBS with revolute clearance joints is the detection of the precise instant of contact between the journal and the bearing. In addition, the numerical model to characterize the contact between the bodies requires the knowledge of the preimpact conditions, that is, the impact velocity and the direction of the plane of collision. The contact duration as well as the penetration cannot be predicted from the preimpact conditions due to the influence of the kinematic constraint imposed by all bodies in the overall system motion. Thus, before the first impact, the journal can freely move inside the bearing and, in this phase, the step size is relatively large and the global configuration of the system is characterized by large translational and rotational displacements. Therefore, the first impact between the journal and the bearing is often made with a high penetration depth, and, consequently, the contact forces are large too. Associated to this overestimated penetration depth between the bodies there are numerical errors that cause inaccurate results.

As it was previously presented, the relative position between the journal and the bearing are given,

$$\boldsymbol{\delta} = e_{ij} - c \tag{30}$$

where e_{ij} is the absolute eccentricity, and c is the radial clearance. Negative values of δ mean that there is no contact between the journal and the bearing. Otherwise, there is contact between the two bodies. Thus, the detection of the instant of contact occurs when the sign of penetration changes between the two discrete moments in time, t and $t + \Delta t$, i.e.,

$$\boldsymbol{\delta}(q(t))^{\mathrm{T}}\, \boldsymbol{\delta}(q(t + \Delta t)) < 0 \tag{31}$$

Therefore, contact is detected when Equation (31) is verified. Such moment in time can be found by using an iterative procedure, such as the Newton-Raphson method.

An alternative way to determine the instant of contact uses the characteristics the integration algorithm selected. Say that during the normal integration procedure the first contact is detected and that the value of the penetration is higher that a prescribed tolerance. In such case the integration time-step is rejected and a new time-step smaller than the previous is tested. The integration process progresses, most probably from a system state for which there is no contact and progresses until contact is detected again. Because the time-step is smaller it is expected that the penetration of this first contact is smaller than the one obtained before. The time-step is rejected until a step is taken, which is within the penetration tolerance. When the 'first' penetration is within the penetration tolerance, it is assumed that such is the moment of the impact and the position and relative velocity of the contact points and the direction of the plane of collision are recorded. It should be highlighted that with this methodology, the step size can reach small values too when compared to the step needed to keep the integration tolerance error under control. Hence, the numerical system can become unstable if the penetration tolerance imposed is too small. In the present work, the contact detection is based on this strategy.

4. Lubricated Revolute Joints

4.1. DYNAMICALLY LOADED JOURNAL-BEARINGS

In most of the machines and mechanisms, the joints are designed to operate with some lubricant fluid. The high pressures generated in the lubricant fluid act to keep the journal and the bearing apart. Moreover, the thin film formed by lubricant reduces friction and wear, provides some load capacity, and adds damping to dissipate undesirable mechanical vibrations. In general, multibody mechanical systems use journal-bearings, in which the load varies in both magnitude and direction, resulting in dynamically loaded journal-bearing. Typical examples of dynamically loaded journal-bearings include the crankshaft bearings in combustion engines, and high-speed turbines bearings supporting dynamic loads caused by unbalanced rotors.

In a broad sense, dynamically loaded journal-bearings can be classified into two groups, namely: squeeze-film action and wedge-film action [31]. The first group refers to the situations in which the journal does not rotate about its center, rather, the journal moves along some path inside the bearing. The second group deals with cases in which there is journal rotation. In a journal-bearing, squeeze-film action is dominant when the relative rotational velocity is small compared to the relative radial velocity. When the relative rotational velocity between the two elements is high the wedge-film effect must also be considered.

Reynolds' equation is used to evaluate the forces developed by the fluid film pressure field. Pinkus and Sternlicht [31], among others, have presented a detailed derivation of the Reynolds' equation, which can be deduced from the Navier-Stokes

equations. The Reynolds' equation involves viscosity, density and film thickness as parameters. By setting fluid density constant, the isothermal generalized Reynolds' equation is [31],

$$\frac{\partial}{\partial X}\left(\frac{h^3}{\mu}\frac{\partial p}{\partial X}\right)+\frac{\partial}{\partial Z}\left(\frac{h^3}{\mu}\frac{\partial p}{\partial Z}\right)=6U\frac{\partial h}{\partial X}+12\frac{dh}{dt} \tag{32}$$

The two terms on the right-hand side of Equation (32) represent the two different effects of pressure generation in the lubricant film, that is, wedge-film action and squeeze-film action, respectively. In the present analysis instead of knowing the applied load, the relative journal-bearing motion characteristics are known and the fluid force from the pressure distribution in the lubricant is the quantity that has to be calculated.

4.2. SQUEEZE-FILM FORCE FOR LONG JOURNAL-BEARINGS

Equation (32) is a nonhomogeneous partial differential of elliptical type. The exact solution of the Reynolds' equation is difficult to obtain, and in general requires considerable numerical effort. It is possible to solve the equation approximately when the first or the second terms on the left-hand side are treated as zero, corresponding the solutions to an infinitely short and an infinitely long journal-bearing, respectively.

For an infinitely long journal-bearing, a constant fluid pressure and negligible leakage in the Z-direction is assumed. In many cases it is possible to treat a journal-bearing as infinitely long and consider only the middle point of it. This approach is valid for length-to-diameter (L/D) ratios greater than 2 [32].

In what follows, the expression for squeeze force of infinite journal-bearings is presented. Squeeze forces are exerted when a fluid is squeezed between two approaching surfaces. In journal-bearing, squeeze-film action is dominant when the relative rotational velocity is small compared to the relative radial velocity, and consequently it is justifiable to drop the wedge-film term in the Reynolds' equation. The objective is to evaluate the resulting force from the given state of position and velocity of the journal-bearing.

In the approximation of an infinitely long journal-bearing, the axial flow is neglected when compared with the circumferential flow; hence the Reynolds' equation reduces to a one dimensional problem and the pressure filed is given by [32]

$$p=\frac{6\mu R_J^3\dot{\varepsilon}}{c^2}\frac{\cos\theta\,(2-\varepsilon\cos\theta)}{(1-\varepsilon\cos\theta)^2} \tag{33}$$

The force f on the journal that must be applied to equilibrate the fluid pressure can be evaluated as an integral of the pressure filed over the surface of the journal yielding,

$$f = \frac{12\pi\mu L R_{\mathrm{J}}^3 \dot{\varepsilon}}{c^2(1-\varepsilon^2)^{\frac{3}{2}}} \tag{34}$$

where μ is the dynamic lubricant viscosity, L is the journal-bearing length, R_J is the journal radius, c is the radial clearance ε is the eccentricity ratio and $\dot{\varepsilon}$ is the time rate of change of eccentricity ratio.

The direction of the force is collinear with the line of centers of the journal and bearing, which is described by the eccentricity vector. Thus, the squeeze force can be introduced into the equation of motion of MBS as generalized force with the journal and bearing centers as points of action for the force and reaction force, respectively. It should be highlighted that the effect of cavitation is not considered in Equation (34), that is, it is assumed that a continuous film exists all around the journal-bearing. However, these conditions are not satisfactory from the physical point of view because the lubricant fluids cannot sustain negative pressures. Based on the mechanics of the journal-bearing of pure squeeze-film action journal-bearing, Ravn [33] includes cavitation effect assuming that negative pressure occurs on the half of journal surface, which faces away from the moving direction.

4.3. MODELING LUBRICATED REVOLUTE JOINTS – HYBRID MODEL

Lubricated revolute joints in MBS do not produce any kinematic constraint like the ideal revolute joints. Instead, they act like a force element producing time dependent forces. Unlike the dry contact model, in a revolute clearance joint with lubricant the gap between the journal and bearing is filled with a lubricant fluid. When there is relative motion between the journal and bearing, the force produced is not zero but depends on the viscosity of the lubricant and the relative position and velocity.

Equation (34), which represents the action on the journal that maintains in equilibrium the field pressure, is valid for situations when the load-capacity of the wedge-film effect is negligible compared to that of the squeeze-film effect. In the squeeze-film lubrication, the journal moves along a radial line in the direction of the applied load, thus, the film thickness decreases and the fluid is forced to flow up around the journal and out the ends of the bearing. Since the squeeze force is proportional to the rate of decrease of fluid film thickness, it is apparent the lubricant acts like a nonlinear viscous damper resisting to the load when the film thickness is decreasing. As the fluid film thickness becomes very thin, that is, the journal is very close to the bearing surface, the force due to the lubricant evaluated from Equation (34) becomes very large. Hence, a discontinuity appears when the film thickness approaches zero, and, consequently, the squeeze force approaches infinity. It is, therefore, assumed that for a certain film thickness, called boundary layer, the fluid can no longer be squeezed out and the journal and bearing wall are considered to be in contact, in a similar way as in the dry contact situation.

The practical criterion for determining whether or not a journal-bearing is operating satisfactorily is the value of the minimum oil film thickness, which is probably the most important parameter in the performance of the journal-bearings. However, it is not easy to establish a unique value of minimum film thickness that can be assumed to be safe since a great deal depends on the manufacturing process, the alignment of the machine elements associated with the journal-bearings, the general operating conditions, including the environment of the machine, amongst others. Moreover, the value of the minimum oil film thickness defines the kind of regime of lubrication is present in the journal-bearing, namely: thick-film lubrication, where the journal-bearing surfaces are totally separated by the lubricant; thin-film lubrication, in which the field of pressure developed, produces elastic deformation. The lubrication between two moving surfaces can shift from one of these two regimes to another, depending on the load, velocity, lubricant viscosity, roughness of surfaces.

For highly loaded contact, the pressure causes elastic deformation of the surfaces, which can be of the same order as the lubricant film thickness. These circumstances are dramatically different from those found in hydrodynamic regime. The contribution of the theory of elasticity with the hydrodynamic lubrication is called Elasto-Hydrodynamic Lubrication theory (EHL).

Figure 8 schematicallyshows the shape of the lubricant film thickness and the pressure distribution within a typical Elasto-Hydrodynamic contact. Due to the normal load P the contacting bodies are deformed. The viscous lubricant, adhering to the surfaces of the moving bodies, is dragged into the high-pressure zone of the contact, therefore, separates the mating surfaces. The pressure distribution within Elasto-Hydrodynamic contact is similar to the dry Hertzian pressure distribution. At the inlet zone, the pressure is slowly built-up until it approximately reaches the maximum Hertzian pressure p. The Elasto-Hydrodynamic lubrication theory goes beyond the scope of the present work.

A hybrid model, which combines the squeeze-film action and the dry contact model, is proposed. Figure 9 showsa partial view of a mechanical system

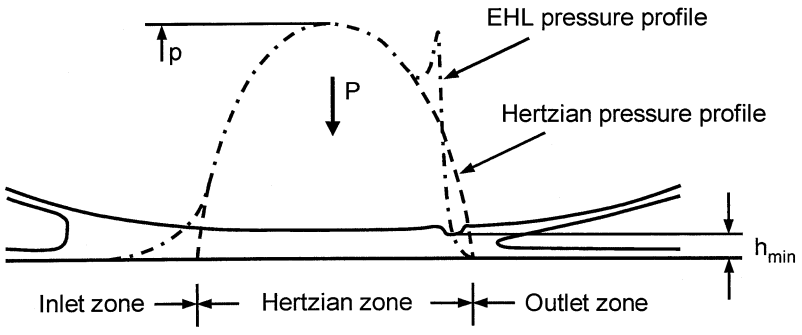

Figure 8. Typical Elasto-Hydrodynamic contact; qualitative shape lubricant film and pressure profile.

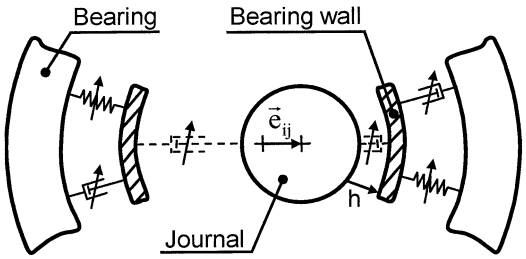

Figure 9. Mechanical system representing a revolute joint with lubricant effect.

representing a revolute clearance joint with lubrication effect, where both the journal and the bearing can have planar motion. The parallel spring-damper element represented by a continuous line refers to the solid-to-solid contact between the journal and the bearing wall, whereas, the damper represented by a dashed line is required only for the lubricated model [34].

If there is no lubricant between the journal and the bearing, the journal can freely move inside the bearing boundaries. When the gap between the two elements is filled with a fluid lubricant, a viscous resistance force exists and opposes to the journal motion. Since the radial clearance is specified, the journal and bearing can work in two different modes:

- Mode 1: the journal and the bearing wall are not in contact with each other and they have a relative radial motion. For the journal-bearing model without lubricant, when $e_{ij} < c$ the journal is in free flight motion and the forces associated to the journal and bearing are null. For lubricated journal-bearing model, the lubricant transmits a force, which must be evaluated from the state variables of the mechanical system.
- Mode 2: the journal and bearing wall are in contact, thus the contact force between the journal and the bearing is modeled as nonlinear Hertz contact law with a hysteresis damping factor.

In short, for a lubricated revolute joint, when the film thickness decreases to the thickness of the boundary layer the model switches from mode 1 to mode 2 and the procedure for the dry contact model is used. After the journal changes direction and the bearing wall deformation return to zero, the model switches back to mode 1.

Since the EHL pressure profile is similar to the Hertzian pressure distribution, it is reasonable to change from squeeze-film action, hydrodynamic lubrication regime, to pure dry contact model. To avoid numerical instabilities and to ensure a smooth transition from pure squeeze-film model to dry contact model, a weighted average is used. When the journal reaches the boundary layer, for which the hydrodynamic theory is not valid, the squeeze-film force model is being substituted by the dry contact force model (seeFigures 10a and 10b).

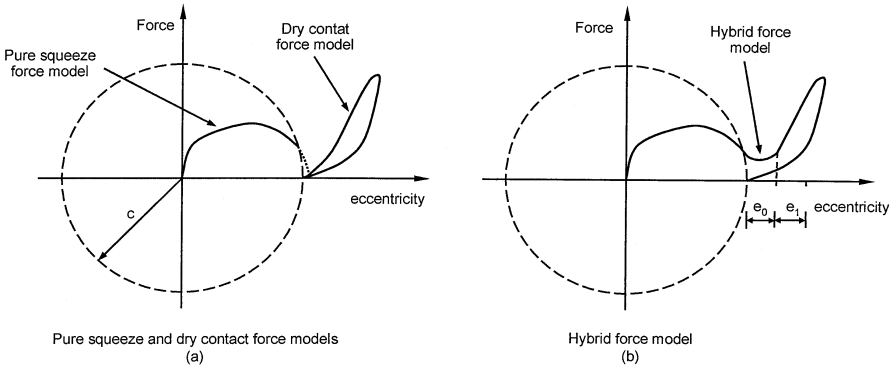

Figure 10. (a) Pure squeeze and dry contact force models; (b) and hybrid force model.

This approach ensures continuity in the joint reaction force, when the squeeze force model is switched to dry contact force model. Mathematically, the hybrid force model is,

$$f = \begin{cases} f_{\text{squeeze}} & \text{if} \quad e \le c \\ \dfrac{(c+e_0)-e}{e_0}\, f_{\text{squeeze}} + \dfrac{e-c}{e_0} f_{\text{dry}} & \text{if} \quad c \le e \le c+e_0 \\ f_{\text{dry}} & \text{if} \quad e \ge c+e_0 \end{cases} \tag{35}$$

where e_0 and e_1 are given tolerances for the eccentricity. The values of these parameters must be chosen carefully, since they depend strongly on the clearance size. It should be noted that the clearance used for the pure squeeze-film force model is not c but it is $c + e_1$ instead.

5. Application Example – Slider–Crank Mechanism

An elementary slider–crank mechanism is used to study the influence of clearance joint models in the dynamic behavior. Figure 11 showsthe configuration of the slider–crank mechanism, which consists of four rigid bodies, that represent the

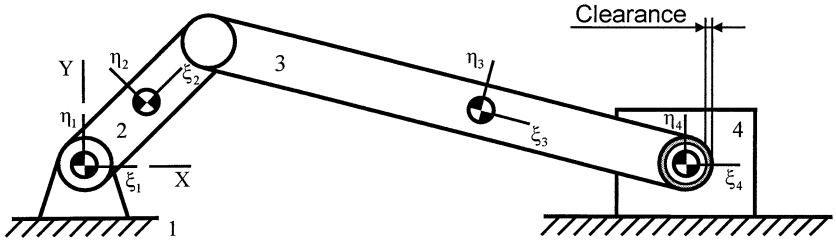

Figure 11. Slider-crank mechanism with a revolute clearance joint.

Table I. Geometric and inertia propertites of slider–crank mechanism.

Body Nr.	Length (m)	Mass (Kg)	Moment of inertia (Kgm^2)
2	0.05	0.30	0.00001
3	0.12	0.21	0.00025
4	–	0.14	–

Table II. Simulation parameters for the slider–crank mechanism.

Bearing radius	10.0 mm	Poisson's ratio	0.3
Journal radius	9.5 mm	Baumgarte – α	5
Restitution coefficient	0.9	Baumgarte – β	5
Friction coefficient	0.03	Integration step size	0.00001 s
Young's modulus	207GPa	Integration tolerance	0.000001

crank, connecting-rod, slider and ground, two ideal revolute joints and one ideal translational joint. A revolute clearance joint exists between the connecting-rod and slider. The length and inertia properties of each body are shown inTable I.

In the dynamic simulation, the crank rotates at constant angular velocity equal to 5000 r.p.m. clockwise. The initial simulation configuration corresponds to the top dead point and the position and velocity journal center are taken to be zero. Initially, the journal and bearing centers coincide.Table II shows the dynamic parameters used in simulation.

Three different situations are analyzed in this work. In the first one, the contact between the journal and the bearing is modeled as dry frictionless contact and the contact force law is given by Equation (25). This model is only valid for colliding spherical surfaces, however, the use is motivated by its simplicity and easiness to implement in a computational program. In the second case, the dry contact is also modeled with Coulomb friction expressed by Equation (28). In the third situation, a hybrid model, that is, a mix between the squeeze force and dry contact force, is used. The behavior of the slider–crank mechanism is quantified by the values of the slider velocity and acceleration, and torque that acts on the crank. In addition, the relative motion between the journal and bearing centers are plotted. The results are provided for two complete crank rotations after steady-state has been reached.

For the first simulation the slider velocity and acceleration are shown inFigure 12(a) and 12(b), respectively. Looking at the velocity curve of the slider, the influence of the joint clearance is clearly observed. The horizontal lines in the velocities correspond to constant slider velocity which occurs when the journal is in free flight motion inside the bearing. Sudden changes in velocity are own to the impact between the journal and bearing, which are visible by the step shaped curve of the velocity diagram. Smooth changes in velocity can also be observed indicating that the journal and the bearing are in continuous contact, i.e., the journal

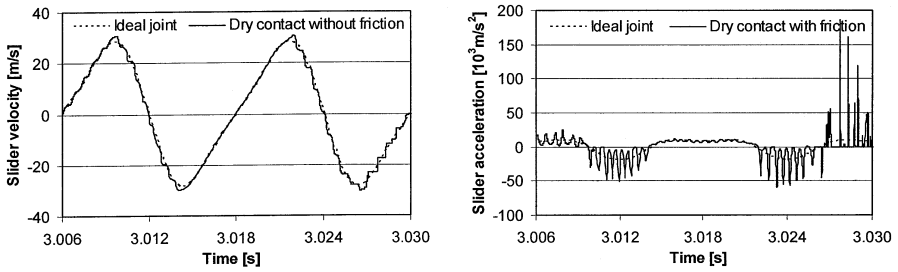

(a) (b)

Figure 12. Velocity (a) and acceleration (b) of the slider for the dry contact model without friction.

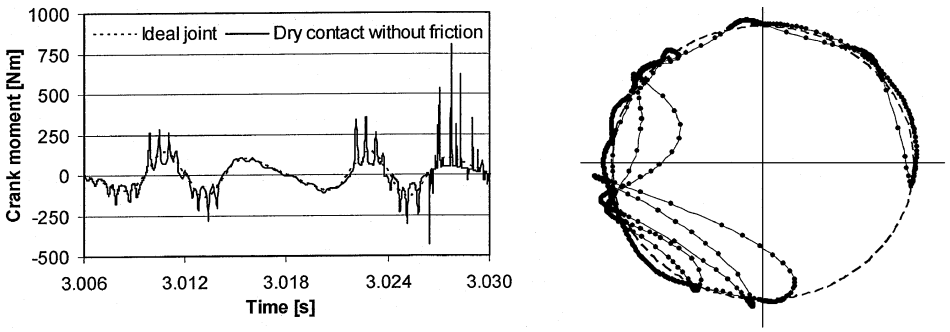

(a) (b)

Figure 13. Crank moment (a) and journal center path (b) for the dry contact model without friction.

follows the bearing wall. This situation is confirmed by smooth changes in the acceleration curve. The impacts between the journal and bearing are visible in the acceleration curve by high peak values, which are immediately followed by null acceleration that correspond to the free flight motion.

The moment applied on the crank to be able to maintain constant, the crank angular velocity is shown inFigure 13(a). The peaks observed on the moment curve are due to the impact forces that are propagated through the rigid bodies of the slider–crank mechanism. The path of the journal center relative to the bearing center is shown in Figure 13(b), where it can be clearly observed the different types of motion between the journal and the bearing, that is, the free flight motion, the impact with rebound, and the continuous contact. The relative penetration depth is visible by the points outside the clearance circle. A point is plotted for each integration time-step. The point density in Figure 13(b) is very high when the journal contacts the bearing, which means that the step size is small. When the journal is in free flight motion the time-step is increased and consequently the dots plotted in the Figure 13(b) are further apart.

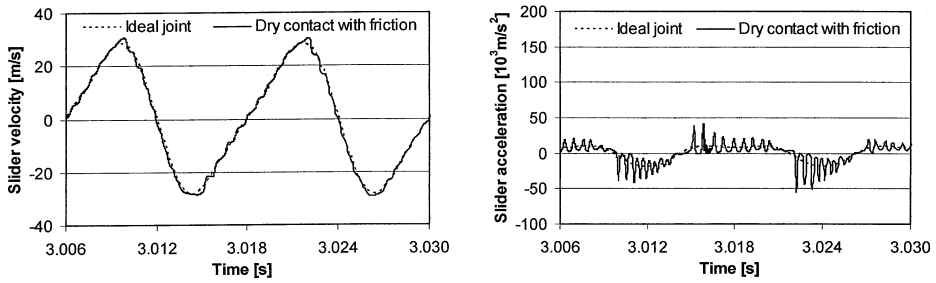

Figure 14. Velocity (a) and acceleration (b) of the slider for the dry contact model with friction.

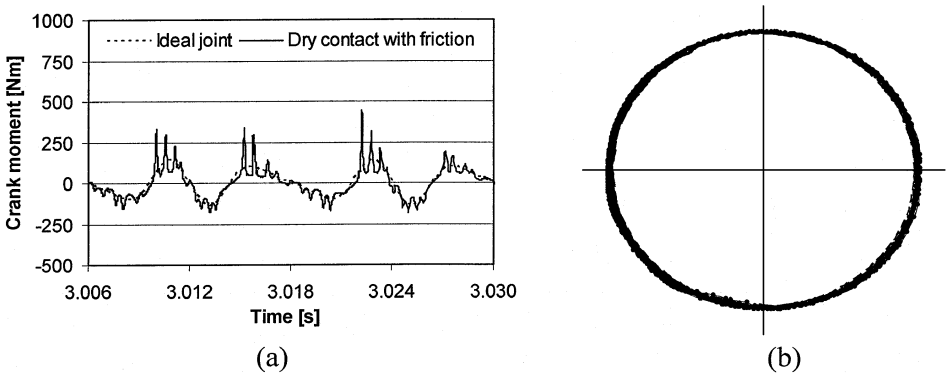

Figure 15. Crank moment (a) and journal center path (b) for the dry contact model with friction.

The second simulation refers to the case, in which the contact between the journal and bearing is modeled by the Lankarani and Nikravesh contact force model together with the Coulomb friction law. In a general, the effect of the friction is to reduce the force peaks due to the impact between the journal and the bearing. This can be observed in the velocity and acceleration slider curves given byFigures 14(a) and 14(b), respectively.Figure 15(b) shows that the path of the journal center is characterized by a continuous contact motion, i.e., the journal follow the bearing wall during all simulation.

The third simulation deals to the case of hybrid model, which combines the squeeze-film action and the dry contact model. The lubricant in the example is a SAE grade 40, which is used in combustion engines. The absolute lubricant viscosity is 400cP. It can be observed in the results for this case, displayedinFigures 16 and 17, that the same qualitative behavior is observed when compared to the case where friction forces are modeled. The lubricant acts like a damper reducing the level of impacts between the journal and bearing.

The overall results are corroborated by published works on this field for the cases that include the dry contact force models [1, 8]. The results obtained with the

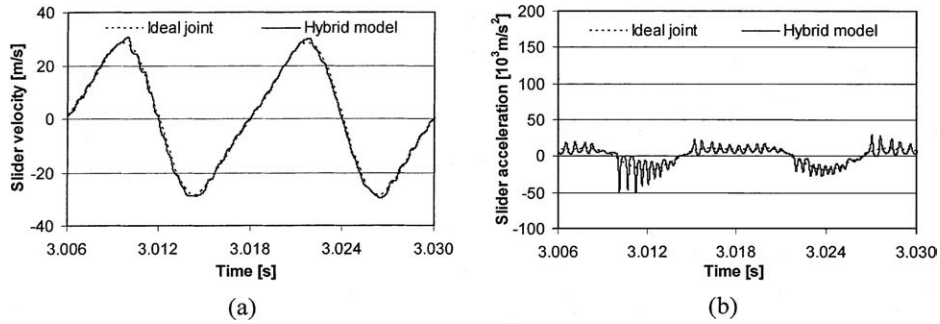

Figure 16. Velocity (a) and acceleration (b) of the slider for the hybrid model.

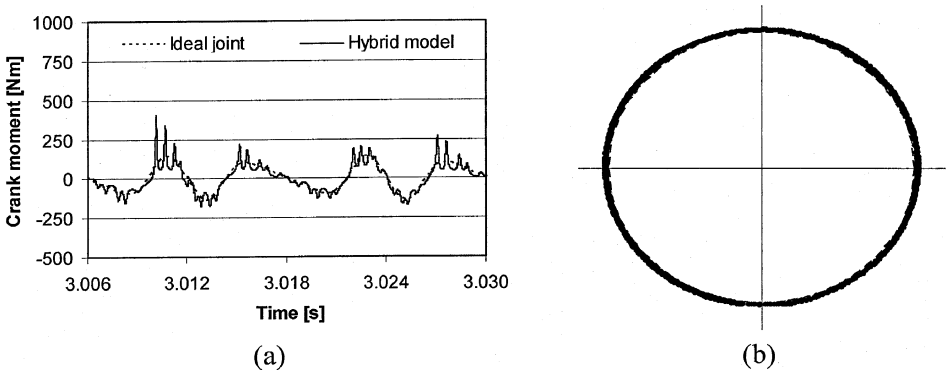

Figure 17. Crank moment (a) and journal center path (b) for the hybrid model.

hybrid model are validated qualitatively by reference to the other models described. Because this is a model proposed for the first time, it is not possible to find in the literature any results that allow for its quantitative validation.

6. Conclusions

A comprehensive approach to the modeling revolute clearance joints in multibody systems has been presented in this work. In the process different contact models have been revised in face of their suitability to represent the impact between the bodies joined by the joint. The methodologies proposed have been exemplified through the application to the dynamics of a slider–crank mechanism with a revolute clearance joint. It was shown that the solution strategy of the contact problem associated with the modeling of joints with clearances is very sensitive to the procedure used to detect contact. In the sequel of the techniques, a numerical strategy compatible with the use of a variable time-step integration algorithm has been proposed to have a time-step selection strategy that is compatible with the identification of the start of contact.

The application of the methodologies proposed to the slider–crank enabled to demonstrate the feasibility of the three contact models proposed. It was shown that the use of the continuous force model, which represents dry contact, when no friction forces are considered lead to unrealistic high peaks in the slider acceleration because the energy dissipation predicted is clearly too low. However, for dry contact model with friction forces or for the hybrid model, the levels of impact force is reduced considerably, and thereby simulate the actual mechanical systems more realistically, when the results are compared with those proposed in the literature. The hybrid model that considers the existence of the lubrication during the free flight of the journal and the possibility for dry contact under some conditions seems to be very well fitted to describe joints with clearances. However, because this is a novel model there are no results in the literature yet that can support this observation.

An important result from this research work is that mechanical systems with clearance joints can have a predictable nonlinear dynamic response and the methodology allows for the calculation of the variation of the driving moments. This is an important feature for the design and control of these systems. The models presented throughout this paper can be used to predict the dynamic response of the machines and mechanisms having clearance joints, namely in what concerns the peak values of impact forces and position and velocity deviations.

Acknowledgements

The authors would like to acknowledge the considerable contributions of Professor Hamid Lankarani of Mechanical Engineering Department of Wichita State University, USA, in the development and implementation of the lubricated joints in mechanical systems. The support of the *Fundação para a Ciência e a Tecnologia* within the project POCTI/EME/2001 Nr 38281 entitled 'Dynamic of Mechanical Systems with Joint Clearances and Imperfections' is gratefully acknowledged.

References

1. Ravn, P., 'A continuous analysis method for planar multibody systems with joint clearance', *Multibody System Dynamics* **2**, 1998, 1–24.
2. Dubowsky, S. and Moening, M.F., 'An experimental and analytical study of impact forces in elastic mechanical systems with clearances', *Mechanism and Machine Theory* **13**, 1978, 451–465.
3. Bahgat, B.M., Osman, M.O.M. and Sankar, T.S., 'On the effect of bearing clearances in the dynamic analysis of planar mechanisms', *Journal of Mechanical Engineering Science* **21**(6), 1979, 429–437.
4. Deck, J.F. and Dubowsky, S., 'On the limitations of predictions of the dynamic response of machines with clearance connections', *Journal of Mechanical Design* **116**, 1994, 833–841.
5. Bengisu, M.T., Hidayetoglu, T. and Akay, A. 'A theoretical and experimental investigation of contact loss in the clearances of a four-bar mechanism', *Journal of Mechanisms, Transmissions, and Automation Design* **108**, 1986, 237–244.

6. Dubowsky, S. and Freudenstein, F., 'Dynamic analysis of mechanical systems with clearances, part 1: Formulation of dynamic model', *Journal of Engineering for Industry*, Series B **93**(1), 1971, 305–309.
7. Dubowsky, S. and Freudenstein, F., 'Dynamic analysis of mechanical systems with clearances, part 2: Dynamic response', *Journal of Engineering for Industry*, Series B **93**(1), 1971, 310–316.
8. Schwab, A.L., 'Dynamics of flexible multibody systems, small vibrations superimposed on a general rigid body motion', Ph.D. Thesis, Delft University of Technology, 2002.
9. Earles, S.W.E. and Wu, C.L.S., 'Predicting the occurrence of contact loss and impact at the bearing from a zero-clearance analysis', *Proceedings of Fourth World Congress on the Theory of Machines and Mechanisms*, Newcastle, England, 1975, 1013–1018.
10. Wu, C.L.S. and Earles, S.W.E., 'A determination of contact-loss at a bearing of a linkage mechanism', *Journal of Engineering for Industry*, Series B **99**(2), 1977, 375–380.
11. Dubowsky, S., 'On Predicting the dynamic effects of clearances in planar mechanisms', *Journal of Engineering for Industry*, Series B **96**(1), 1974, 317–323.
12. Townsend, M.A. and Mansour, W.M., 'A pendulating model for mechanisms with clearances in the revolutes', *Journal of Engineering for Industry*, Series B **97**(1), 1975, 354–358.
13. Nikravesh, P.E., *Computer-Aided Analysis of Mechanical Systems*, Prentice Hall, Englewood Cliffs, NJ, 1988.
14. Garcia de Jalon, J. and Bayo, E., *Kinematic and Dynamic Simulations of Multibody Systems*, Springer-Verlag, New York, 1994.
15. Baumgarte, J., 'Stabilization of constraints and integrals of motion in dynamical systems', *Computer Methods in Applied Mechanics and Engineering* **1**, 1972, 1–16.
16. Shampine, L. and Gordon, M., *Computer Solution of Ordinary Differential Equations: The Initial Value Problem*, Freeman, San Francisco, 1975.
17. Lankarani, H.M. and Nikravseh, P.E., 'A contact force model with hysteresis damping for impact analysis of multibody systems', *Journal of Mechanical Design* **112**, 1990, 369–376.
18. Miedema, B. and Mansour, W.M., 'Mechanical joints with clearance: A three-mode model', *Journal of Engineering for Industry*, Series B **98**(4), 1976, 1319–1323.
19. Haines, R.S., 'Survey: 2-dimensional motion and impact at revolute joints', *Mechanism and Machine Theory* **15**(5), 1980, 361–370.
20. Zukas, J.A., Nicholas, T., Greszczuk, L.B. and Curran, D.R., *Impact Dynamics*, John Wiley, New York, 1982.
21. Timoshenko, S.P. and Goodier, J.N., *Theory of Elasticity*, McGraw-Hill, New York, 1970.
22. Goldsmith, W., *Impact, The Theory and Physical Behaviour of Colliding Solids*, Edward Arnold Ltd, London, England, 1960.
23. Hunt, K.H. and Crossley, F.R., 'Coefficient of restitution interpreted as damping in vibroimpact', *Journal of Applied Mechanics* **7**, 1975, 440–445.
24. Love, A.E.H., *A Treatise on the Mathematical Theory of Elasticity*, 4th edn. Dover Publications, New York, 1944.
25. Lankarani, H.M. and Nikravesh, P.E., 'Continuous contact force models for impact analysis in multibody systems', *Nonlinear Dynamics* **5**, 1994, 193–207.
26. ESDU-78035 Tribology Series, *Contact Phenomena. I: Stresses, Deflections and Contact Dimensions for Normally-Loaded Unlubricated Elastic Components*, Engineering Sciences Data Unit, London, England, 1978.
27. Greenwood, D.T., *Principles of Dynamics*, Prenctice-Hall, Englewood Cliffs, NJ, 1965.
28. Bagci, C., 'Dynamic motion analysis of plane mechanisms with coulomb and viscous damping via the joint force analysis', *Journal of Engineering for Industry*, Series B **97**(2), 1975, 551–560.
29. Haug, E.J., Wu, S.C. and Yang, S.M., 'Dynamics of mechanical systems with coulomb friction, stiction, impact and constraint addition-deletion – I theory', *Mechanism and Machine Theory* **21**(5), 1986, 401–406.

30. Ambrósio, J., Impact of rigid and flexible multibody systems: Deformation description and contact models, in *Virtual Nonlinear Multibody Systems*, (Michael Valasek, Werner Schiehlen, eds.), Kluwer Academic Publishers, Dordrecht, Netherlands, 2003, 57–81.
31. Pinkus, O. and Sternlicht, S.A., *Theory of Hydrodynamic Lubrication*, McGraw-Hill, New York, 1961.
32. Hamrock, B.J., *Fundamentals of Fluid Film Lubrication*, McGraw-Hill, New York, 1994.
33. Ravn, P., 'Analysis and synthesis of planar mechanical systems including flexibility, contact and joint clearance', Ph.D. Thesis, DCAMM Report No. S78, Technical University of Denmark, 1998.
34. Roger, R.J., Andrews, G.C., 'Dynamic simulation of planar mechanical systems with lubricated bearing clearances using vector-network methods', *Journal of Engineering for Industry*, Series B **99**(1), 1977, 131–137.